ISSN 0974-3618 (Print)
0974-360X (Online)

www.rjptonline.org

RESEARCH ARTICLE

Computational Study on Molecular Structure, UV-Visible and Vibrational Spectra and Frontier Molecular Orbital Analysis of (E)-7-((2-Chloroquinolin-3-yl)methylene)-1,2,6,7-tetrahydro-8*H*-indeno[5,4-b]furan-8-one

Vishnu A. Adole[1]*, Abhijit R. Bukane[1], Ravindra H. Waghchaure[2], Rohit S. Shinde, Bapu S. Jagdale[1]

[1]Department of Chemistry, Mahatma Gandhi Vidyamandir's Arts, Science and Commerce College, Manmad, Nashik - 423104, India (Affiliated to SP Pune University, Pune)

[2]Department of Chemistry, Mahant Jamanadas Maharaj Arts, Commerce and Science College, Karanjali, Taluka - Peth, District – Nashik - 422 208, India (Affiliated to SP Pune University, Pune)

*Corresponding Author E-mail: **vishnuadole86@gmail.com**

ABSTRACT:

Quinoline scaffold is one of the most often perceived parts in biologically active organic compounds. In light of this, an quinoline containing 2-arylidene derivative; (*E*)-7-((2-chloroquinolin-3-yl)methylene)-1,2,6,7-tetrahydro-8*H*-indeno[5,4-b]furan-8-one (2-CQMIF) is studied by using density functional theory (DFT) at B3LYP/6-311G(d,p) basis set. The geometry of the 2-CQMIF molecule was optimized by using B3LYP/6-311G(d,p) basis set and in-depth structural analysis on bond lengths and bond angles has been discussed. The frontier molecular orbital (FMO) analysis and various quantum chemical parameters are calculated and discussed for the better understanding of chemical behavior of the title molecule. The theoretical and experimental UV-Visible absorption bands are compared. The TD-DFT method at B3LYP/6-311G(d,p) basis set was employed to predict the electronic excitations. The scaled theoretical vibrational assignments calculated at 6-311G(d,p) level are compared with the experimental results and the good agreement is observed between them. Molecular electrostatic potential (MEP) surface investigation is presented to understand the reactivity sites of the title molecule. Besides, some thermodynamic properties have also been computed at same level of theory.

KEYWORDS: B3LYP/6-311G(d,p), Quinoline, Time Dependent DFT, HOMO-LUMO.

INTRODUCTION:

Quinoline is a bicyclic heterocyclic moiety with massive remedial potential. Quinolines are known for their excellent antimalarial[1-3], anti-inflammatory[4], analgesic[5], antibacterial[6], antifungal[7], anticancer[8,9], antiviral[10], anthelmintic[11], antiprotozoal[12], and other miscellaneous biological activities[13,14]. Some quinoline derivatives have also been used in the treating erectile dysfunction [15], and Alzheimer's disease[16].

Likewise 2-arylidene indanone skeleton has also received tremendous attention of the medicinal chemists due to its involvement in various applications. The diverse biological profile of compounds containing 2-arylidene indanone skeleton includes properties like antimalarial1[7] antioxidant[18] antimicrobial[19] anti-inflammatory[20], etc. The structure of 2-arylidene indanone is similar to chalcones. Chalcones act as vital intermediates in synthetic organic chemistry, and additionally, they are found to show powerful and many biological properties[21]. The noteworthy biological activities shown by chalcones include anti-tubercular[22], antihypertensive[23], antioxidant[24], anticancer[25], antiviral[26], antimicrobial[27], etc.

Received on 24.01.2021 Modified on 20.05.2021
Accepted on 30.07.2021
Research J. Pharm.and Tech 2022; 15(3):1101-1108.
DOI: 10.52711/0974-360X.2022.00184

Green chemistry based organic synthesis has expanded tremendously in past few years[28-37]. Researchers are currently focusing on development of green strategies for the synthesis of organic compounds of biological importance[38,39]. Theoretical chemistry calculations are dependent on physicochemical calculations and quantum chemistry. DFT can predict various molecular properties. Especially, different spectroscopic investigations can be achieved: UV/Vis spectra, IR and Raman frequencies and intensities, NMR chemical shifts, and spin-spin coupling constants[40-44]. Likewise, DFT calculations can predict HOMO-LUMO energies, bond lengths, bond angles, dihedral angles, and spectroscopic properties[45-66]. The comparison of theoretical calculations with experimental results provides good deal of information. By using computation results, it has become possible to arrive at reaction mechanistic pathway. DFT method via B3LYP functional has been shown to predict theoretical properties that agree well with experimental spectroscopic findings[67-74]. The assignment of absorption bands and, as a result, the prediction of electronic and chemical properties of molecules is found to be accurate when using the B3LYP functional with a 6-311G(d,p) basis package[49,75, 76]. In light of various aspects discussed above, here in this paper, we wish to report density functional theory investigation of previously synthesized (*E*)-7-((2-chloroquinolin-3-yl)methylene)-1,2,6,7-tetrahydro-8*H*-indeno[5,4-*b*]furan-8-one[32] (2-CQMIF). To the best of our knowledge, this the first report on computational study of the title molecule.

METHODS:

Computational study:

DFT calculations were performed on an Intel (R) Core (TM) i5 computer using Gaussian-03 program package without any constraint on the geometry[77]. The geometry of the molecules studied in this is optimized by DFT/B3LYP method using 6-311G(d,p) basis set. The FMO analysis and quantum chemical study was performed using same basis set. The electronic excitations of title molecule have been calculated at TD-B3LYP/6-311G(d,p) level of theory for B3LYP/6-311G(d,p) optimized geometries. To investigate the reactive sites of the title molecules, the MEP was computed using the same method. All the calculations were carried out for the optimized structure in the gas phase. The experimental UV-Visible spectrum is recorded in dimethyl sulfoxide (DMSO) solvent.

RESULTS AND DISCUSSION:

Optimized Molecular Structure:

The optimized molecular structure of the title 2-CQMIF molecule is given in Figure 1. In Figure 2, the optimized molecular structures are presented along x,y and z Cartesian axes. The 2-CQMIF molecule is having C1 point group symmetry and the dipole moment is 5.0279 Debye. The optimized geometrical parameters; bond lengths and bond angles of the title molecule have been computed and presented here in Table 1 and Table 2. In the 2-CQMIF molecule, the C=O (C16-O20) bond length is 1.2169 Å and the C=C (C21-C22) bond length in alkene is 1.3453 Å. The C-Cl (C26-Cl35) bond length is 1.7713 Å. The imine bond lengths are 1.2912 Å (C26-N34) and 1.3639 Å (C27-N34). Amongst aromatic C=C bond lengths, C32-C36 bond is the longest (1.4148 Å) and the shortest is C30-C32 (1.3741 Å). Other bond lengths are also in good agreement. All the bond angles are also in good agreement.

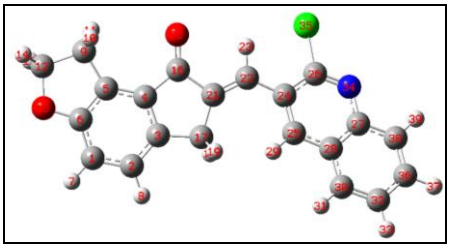

Figure 1 Optimized molecular structure of 2-CQMIF molecule

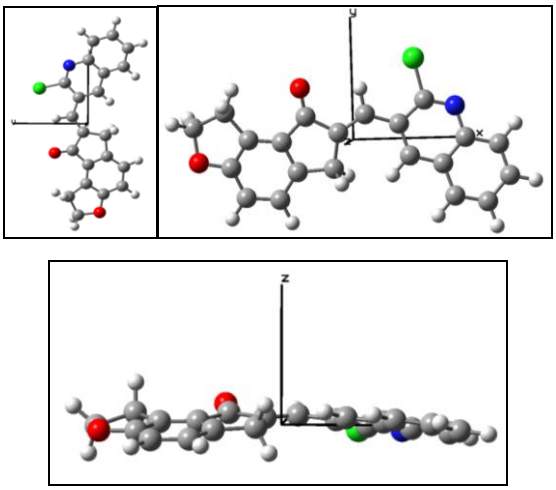

Figure 2 Optimized molecular structures along x, y and z Cartesian axes

Table 1 Optimized geometrical parameters of 2-CQMIF molecule at B3LYP/6-311G(d,p) basis set

Bond lengths (Å)					
C1-C2	1.3988	C9-C12	1.547	C25-C28	1.4115
C1-C6	1.3946	C12-H13	1.0937	C25-H29	1.0815
C1-H7	1.083	C12-H14	1.0892	C26-N34	1.2912
C2-C3	1.3912	C12-O15	1.4586	C26-Cl35	1.7713
C2-H8	1.0849	C16-O20	1.2169	C27-H28	1.4247
C3-C4	1.4025	C16-C21	1.5051	C27-N34	1.3639
C3- C17	1.518	C17-H18	1.0964	C27-H38	1.4137
C4- C5	1.3884	C17-H19	1.097	C28-C30	1.4182
C4-C16	1.4785	C17-C21	1.5144	C30-H31	1.0849
C5- C6	1.3918	C21-C22	1.3453	C30-C32	1.3741
C5- C9	1.5068	C22-H23	1.0853	C32-H33	1.0838
C6- O15	1.3609	C22-C24	1.4587	C32-C36	1.4148
C9-H10	1.0947	C24-C25	1.3852	C36-H37	1.084
C9-H11	1.0908	C24-C26	1.4412	C36-C38	1.3756
-	-	-	-	C38-H39	1.0828

Table 2 Optimized geometrical parameters of 2-CQMIF molecule at B3LYP/6-311G(d,p) basis set

Bond angles (°)					
C2-C1-C6	118.6792	C9-C12-H14	114.0114	C24-C25-H29	119.831
C2-C1-H7	121.3271	C9-C12-O15	106.9746	C28-C25-H29	118.3896
C6-C1-H7	119.9937	H13-C12-H14	109.1494	C24-C26-H34	125.9158
C1-C2-C3	119.8758	H13-C12-O15	107.4423	C24-C26- C35	118.8301
C1-C2-H8	119.3895	H14-C12-C15	107.3166	C34-C26- C35	115.2504
C3-C2-H8	120.7338	C6-O15-C12	107.3502	C28-C27-H34	121.282
C2-C3-C4	120.2855	C4-C16-O20	127.2201	C28-C27-H38	119.5377
C2-C3-C17	128.6913	C4-C16-C21	106.2361	C34-C27-H38	119.1801
C4-C3-C17	111.0177	O20-C16-C21	126.5389	C25-C28-H27	117.4084
C3-C4-C5	120.5697	C3-C17-H18	112.3595	C25-C28-C30	123.4341
C3-C4-C16	110.0995	C3-C17-H19	110.3293	H27-C28-C30	119.1569
C5-C4-C16	129.3255	C3-C17-C21	103.7193	C28-C30-C31	119.1525
C4-C5-C6	118.2778	H18-C17-H19	106.8224	C28-C30-C32	120.2186
C4-C5-C9	133.1514	H18-C17-C21	111.8902	C31-C30-C32	120.6289
C6-C5-C9	108.5203	C19-C17-C21	111.8123	C30-C32-H33	120.0798
C1-C6-C5	122.3103	C16-C21-C17	108.8148	C30-C32-H36	120.4003
C1-C6-O15	124.3643	C16-C21-H22	119.1896	C33-C32-H36	119.5198
C5-C6-O15	113.3246	C17-C21-H22	131.8969	C26-C34-H27	118.9995
C5-C9-H10	110.6353	C21-C22-H23	114.2978	C32-C36-H37	119.4032
C5-C9-H11	113.058	C21-C22-C24	129.6375	C32-C36-H38	120.7067
C5-C9-C12	101.1396	H23-C22-C24	116.0475	C37-C36-H38	119.8901
H10-C9-H11	107.0772	C22-C24-C25	123.8786	C27-C36-H38	119.9795
H10-C9-C12	112.2751	C22-C24-C26	121.483	C27-C36-H39	117.9387
H11-C9-C12	112.7172	C25-C24-C26	114.6289	C38-C38- C39	122.0818
C9-C12-H13	111.6315	C24-C25-C28	121.7644	-	-

Global descriptor analysis:

The pictorial representation of HOMO-LUMO orbitals is given in Figure 3. The electronic parameters such as E_{HOMO}, E_{LUMO}, ionization enthalpy (I), and electron affinity are given in Table 3. The quantum chemical parameters like electronegativity (χ), absolute hardness (η), softness (σ), electrophilicity (ω), chemical potential (Pi) are presented in Table 4. The frontier molecular orbital (FMO) analysis suggests that the energy gap in the 2-CQMIF molecule is 3.4626 eV. The lower HOMO-LUMO energy gap demonstrates the inevitable charge transfer is happening within the molecule. The global softness (σ), and the absolute hardness (η) values are 1.7313 eV and 0.5776 eV respectively. The ease of removal of an electron is governed by its chemical potential Pi and it is likewise identified with its electronegativity (χ). A good electrophile is described by a higher value of global electrophilicity (ω) and the higher value of ω indicates good nucleophile. Our results suggest that the 2-CQMIF molecule has a higher value of global electrophilicity (ω = 5.2948 eV), so it is most likely to accept electrons readily and also would undergo nucleophilic attack easily. As Pi value increases, the ability of a molecule to lose an electron increases. The maximum charge transfer is in the title molecule is 2.5673 eV.

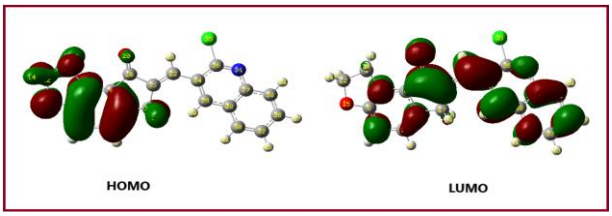

Figure 3 HOMO-LUMO pictures

Table 3 Electronic parameters of 2-CQMIF molecule

Parameter	**Values**
E (a.u.)	−1474.33
E_{HOMO} (eV)	−6.1761
E_{LUMO} (eV)	−2.7135
I (eV)	6.1761
A (eV)	2.7135
Eg (eV)	3.4626

Table 4 Global reactivity parameters of 2-CQMIF molecule

Parameter	**Values**
χ (eV)	4.4448
η (eV)	1.7313
σ (eV^{-1})	0.5776
ω (eV)	5.7056
Pi (eV)	−4.4448
ΔNmax (eV)	2.5673
Dipole Moment (Debye)	5.0279

UV-Visible study:

The theoretical UV-Visible spectral study of 2-CQMIF molecule were performed at TD-DFT-B3LYP method with 6-311G(d,p) basis set. The theoretical UV-Visible simulation was carried out in gas phase and DMSO. The experimental UV-Visible spectrum was recorded in DMSO solvent. The theoretical and experimental UV-Visible spectra are depicted in Figure 4 and Figure 5

respectively. The computed UV-Visible data is compared with the experimental observations for the assignment of absorption signals. The UV-Visible computations were simulated up to three singlet excited states. The gas phase theoretical UV-Visible absorption signals are found at 400.39nm, 377.53nm, and 335.22 nm. The absorption peak at 400.39nm arises due to the n-π* transition. The other two peaks are comparatively more intense peaks and therefore arise due to the π - π* transitions. The theoretical UV-Visible spectrum in the DMSO solvent exhibited peaks at 388.77nm, 384.33 nm and 347.58nm for the first three singlet excited states. This infers that DMSO has hypsochromic shift on the first excited state and bathochromic shift on the second and third singlet excited states. This validates the correct assignment of the absorption bands. The experimental values for the absorption peaks are 384.25 nm and 337.12nm. These two peaks are rightly matching with the first and third singlet excited states recorded theoretically in DMSO solvent.

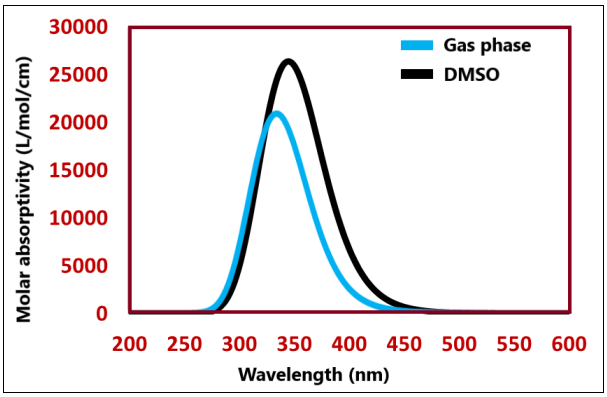

Figure 4 Simulated UV-Visible spectra of 2-CQMIF in gas phase and DMSO

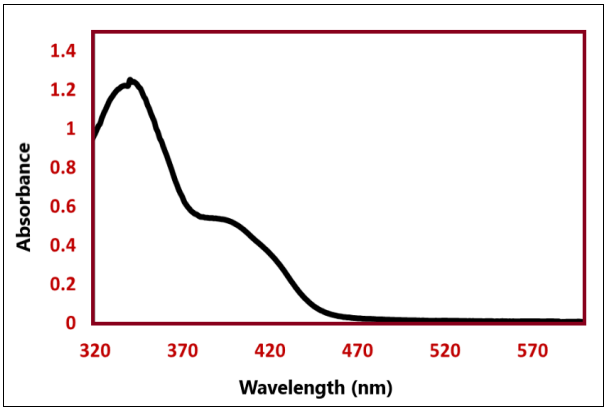

Figure 5 Experimental UV-Visible spectrum of CQMIF in DMSO

Mulliken atomic charges:

The Mulliken atomic charges of the 2-CQMIF molecule are calculated by DFT/B3LYP method with 6-311G(d,p) basis set in the gaseous phase and are given in Table 5 and pictorial representation is given in Figure 6. Mulliken atomic charges reveal that all the hydrogen atoms have a net positive charge but H18 and H19 atoms have a more positive charge than other hydrogen atoms and therefore they are more acidic. These two hydrogen atoms are flanked between two C=C groups. Amongst, a carbon atom, the C6 atom has the highest net positive charge (0.238699) as it is attached to an electronegative oxygen atom. On the other hand C21 atom has the highest negative charge (-0.212075).

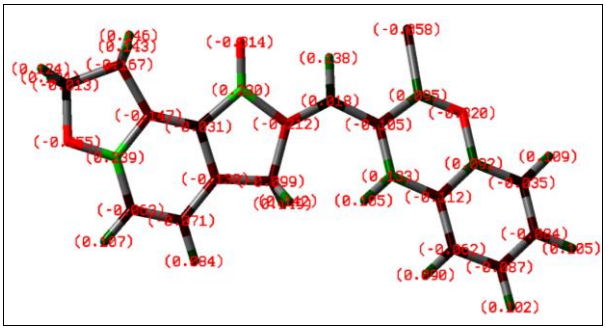

Figure 6 Mulliken atomic charge distribution in 2-CQMIF molecule

Table 5 Mulliken atomic charges in 2-CQMIF molecule

Atom	Charge	Atom	Charge
1 C	-0.063438	21 C	-0.212075
2 C	-0.071060	22 C	0.017836
3 C	-0.138021	23 H	0.137538
4 C	-0.031269	24 C	-0.104750
5 C	-0.146792	25 C	0.133430
6 C	0.238699	26 C	0.095249
7 H	0.106805	27 C	0.091854
8 H	0.083850	28 C	-0.112266
9 C	-0.167357	29 H	0.105150
10 H	0.142645	30 C	-0.062353
11 H	0.146102	31 H	0.090465
12 C	-0.012783	32 C	-0.087285
13 H	0.123688	33 H	0.102484
14 H	0.123675	34 N	-0.320277
15 O	-0.354584	35 Cl	-0.058044
16 C	0.229659	36 C	-0.084241
17 C	-0.098668	37 H	0.104824
18 H	0.148561	38 C	-0.035129
19 H	0.142213	39 H	0.109330
20 O	-0.313665	-	-

Vibrational Assignments:

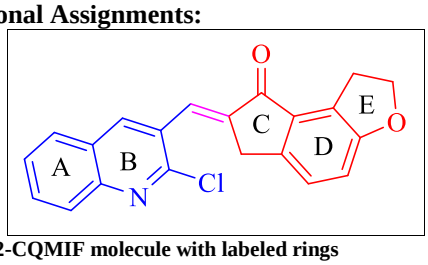

Figure 7 2-CQMIF molecule with labeled rings

The titled 2-CQMIF molecule has 39 atoms and therefore has 111 fundamental modes of vibration according to 3N–6 formula. The 2-CQMIF molecule has labeled according rings present in it (Figure 7).

Essentially all 111 fundamental modes of vibrations are IR active. The harmonic-vibrational frequencies calculated for a molecule at B3LYP level using basis set 6-311G(d,p) have been represented in Table 6. The comparison has been made between observed frequencies with scaled frequencies DFT hybrid B3LYP method, and it has been found that there is good agreement between scaled and experimental frequencies. Computed harmonic vibrational wavenumbers are usually higher than experimental ones owing to the anharmonicity of the incomplete treatment of electron correlation[78]. 6-311G(d,p) basis set was used to determine harmonic frequencies, which were then scaled by an acceptable scaling factor[49,79].

Table 6 Selected experimental and scaledtheoretical vibrational assignments of 2-CQMIF molecule calculated at B3LYP/6-311G(d,p) level

Mode	Computed scaled frequencies (cm^{-1})	IR Intensity (km) mol^{-1}	Observed frequencies (cm^{-1})	Assignments
110	3196.23	9.74	-	*ν* C-H (Ring A)
109	3193.24	1.67	-	*ν* C22-H
107	3189.33	2.43	-	*ν* C1-H, C2-H
106	3182.212	26.07	-	ν asym C9-H_2, ν asym C12-H_2
100	3127.53	8.49	-	*ν* sym C9-H_2
99	3117.72	55.12	-	ν sym C12-H_2
98	3092.74	7.82	-	ν sym C17-H2
96	1626.98	26.04	1620.21	*ν* C=C (Ring D)
95	1602.06	16.04	-	*ν* C=C (ring D)
93	1546.38	104.51	-	*ν* C=C (C21-C22)
91	1503.24	17.40	1473.62	*ν* C=C (Ring B), *ν* C=C (C21-C22)
84	1365.53	48.53	1338.60	β C25-H, □-C17-H_2
79	1259.22	0.88	1253.73	□□-C12-H_2
77	1225.18	10.96	1230.58	β C22-H
73	1157.92	0.73	1139.93	t-C9-H_2, t-C12-H_2, β C1-H, β C2-H
58	924.78	33.57	929.69	□□C9-H_2
52	868.06	1.22	864.11	γ C1-H, γ C2-H
48	836.14	10.02	819.75	t-C12-H_2
46	776.28	33.56	771.53	β-H (Ring A)
38	684.67	5.50	684.73	γ C1-H, γ C22-H, γ C30-H, γ C39-H, Ring A,B,C, D, E def

v- stretching; sym- symmetric; asym- asymmetric; def- deformation; β- In-plane bending; γ- Out of plane bending; ρ- rocking; t- twisting; □- wagging; □- scissoring

Thermodynamic properties:

The thermodynamic data of 2-CQMIF molecule obtained from DFT method at B3LYP/6-311G(d, p) level is presented in Table 7. Here in this, E_{total}, Heat Capacity at constant volume, total entropy S, zero point vibrational Energy and Rotational constants have been presented. The data revealed in this could be useful for the further assessment of the other thermodynamic properties.

Table 7 Thermodynamic properties of the title molecule

Parameter	Value
E total (kcal mol^{-1})	194.867
Translational	0.889
Rotational	0.889
Vibrational	193.090
Heat Capacity at constant volume, Cv (cal $mol^{-1}K^{-1}$)	74.163
Translational	2.981
Rotational	2.981
Vibrational	68.202
Total entropy S (cal $mol^{-1}K^{-1}$)	131.895
Translational	43.427
Rotational	35.877
Vibrational	52.591
Zero point Vibrational Energy Ev_0 (kcal mol^{-1})	184.02385
Rotational constants (GHZ)	0.41718
	0.09596
	0.07870

Molecular electrostatic potential surface analysis:

MEP plot is given in Figure 8. The phenomena like nucleophilic and electrophilic sites, solvent effects, hydrogen bonding interactions, etc. could be determined by the use of a molecular electrostatic potential. MEP is primarily used to find out the reactive sites of molecules empower to anticipate how one particle can interact with other molecules. The different values of the electrostatic potential at the surface of the molecule are represented by distinct colours. The red and yellow regions correspond to the region of high electron density and are associated with electrophilic reactivity. On the other hand, the blue parts represent low electron density and susceptible to nucleophilic reactivity and green colours represent regions of zero potential, respectively. The MEP surface analysis indicates that the benzene ring attached to the dihydrofuran ring is highly susceptible to aromatic electrophilic substitution reactions and quinoline moiety is prone to nucleophilic attacks.

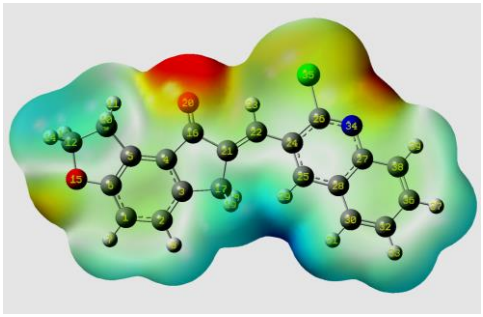

Figure 8. Molecular electrostatic potential

CONCLUSIONS:

In conclusion, structural, chemical and spectroscopic aspects of titled compound 2-CQMIF have been explored by utilizing DFT strategy at B3LYP/6-311G(d,p), and TD-DFT at B3LYP/6-311G(d,p) basis

set. The molecule title molecule is having C1 point group symmetry and the dipole moment is 5.0279 Debye. Structural parameters are examined to comprehend understand the chemical structure of the title molecule. The lower energy gap in the titled molecule demonstrates the inevitable charge transfer is happening within the molecule. Our results suggest that the title molecule is most likely to accept electrons promptly and furthermore would go through nucleophilic attack easily. The comparison between the theoretical and experimental spectral analysis shows good agreement. The investigation uncovered that the first singlet excited state arises due to the n-π^* transition. The MEP surface analysis shows that the benzene fused to dihydrofuran ring is highly susceptible to aromatic electrophilic substitution reactions and quinoline structure is prone to nucleophilic attacks. This study could provide a ladder for the further exploration of the title molecule in various fields.

ACKNOWLEDGEMENT:

Authors are grateful to Prof. (Dr.) A. B. Sawant for his guidance for the Gaussian study. Authors acknowledge Department of Chemistry, Arts, Science and Commerce College, Manmad, MS, India for research facilities.

CONFLICT OF INTEREST:

The authors declare no conflict of interest.

REFERENCES:

1. Chibale K, Moss JR, Blackie M, van Schalkwyk D, Smith PJ. New amine and urea analogs of ferrochloroquine: Synthesis, antimalarial activity in vitro and electrochemical studies. Tetrahedron Letters. 2000; 41(32): 6231-6235.
2. Singh B, Chetia D, Puri SK, Srivastava K, Prakash A, Synthesis and in vitro and in vivo antimalarial activity of novel 4-anilinoquinoline Mannich base derivatives. Medicinal Chemistry Research. 2011; *20*(9): 1523-1529.
3. Bhat HR, Singh UP, Gahtori P, Ghosh SK, Gogoi K, Prakash A, Singh RK. Antimalarial activity and docking studies of novel bi-functional hybrids derived from 4-aminoquinoline and 1,3,5-triazine against wild and mutant malaria parasites as pf-DHFR inhibitor. RSC Advances. 2013; 3(9): 2942-2952.
4. Gilbert AM, Bursavich MG, Lombardi S, Georgiadis KE, Reifenberg E, Flannery CR, Morris EA. N-((8-Hydroxy-5-substituted-quinolin-7-yl)(phenyl) methyl)-2-phenyloxy/amino-acetamide inhibitors of ADAMTS-5 (Aggrecanase-2). Bioorganic & Medicinal Chemistry Letters. 2008; 18(24): 6454-6457.
5. Elsayed Khidre R, Fathy Abdel-Wahab B, Abdel-Rehem Badria F. New quinoline-based compounds for analgesic and anti-inflammatory evaluation. Letters in Drug Design & Discovery. 2011; 8(7):640-648.
6. Fu HG, Li ZW, Hu XX, Si SY, You XF, Tang S, Wang YX, Song DQ. Synthesis and biological evaluation of quinoline derivatives as a novel class of broad-spectrum antibacterial agents. Molecules. 2019; 24(3): 548.
7. Musiol R, Jampilek J, Buchta V, Silva L, Niedbala H, Podeszwa B, Palka A, Majerz-Maniecka K, Oleksyn B, Polanski J. Antifungal properties of new series of quinoline derivatives. Bioorganic & Medicinal Chemistry. 2006; 14(10): 3592-3598.
8. Nasr EE, Mostafa AS, El-Sayed MA, Massoud MA. Design, synthesis, and docking study of new quinoline derivatives as antitumor agents. Archiv der Pharmazie. 2019; 352(7): 1800355.
9. Marganakop SB, Kamble RR, Hoskeri J, Prasad DJ, Meti GY. Facile synthesis of novel quinoline derivatives as anticancer agents. Medicinal Chemistry Research. 2014; 23(6): 2727-2735.
10. De la Guardia C, Stephens DE, Dang HT, Quijada M, Larionov OV, Lleonart R. Antiviral activity of novel quinoline derivatives against dengue virus serotype 2. Molecules. 2018; 23(3): 672.
11. Rossiter S, Peron JM, Whitfield PJ, Jones K. Synthesis and anthelmintic properties of arylquinolines with activity against drug-resistant nematodes. Bioorganic & Medicinal Chemistry Letters. 2005; 15(21): 4806-4818.
12. Hochegger P, Faist J, Seebacher W, Saf R, Mäser P, Kaiser M, Weis R. Antiprotozoal Activities of Tetrazole-quinolines with Aminopiperidine Linker. Medicinal Chemistry. 2019; 15(4): 409-416.
13. Marella A, Tanwar OP, Saha R, Ali MR, Srivastava S, Akhter M, Shaquiquzzaman M, Alam MM. Quinoline: A versatile heterocyclic. Saudi Pharmaceutical Journal. 2013; 21(1): 1-2.
14. Hussaini SM. Therapeutic significance of quinolines: a patent review (2013-2015). Expert Opinion on Therapeutic Patents. 2016; 26(10): 1201-1221.
15. Bi Y, Stoy P, Adam L, He B, Krupinski J, Normandin D, Pongrac R, Seliger L, Watson A, Macor JE. Quinolines as extremely potent and selective PDE5 inhibitors as potential agents for treatment of erectile dysfunction. Bioorganic & Medicinal Chemistry Letters. 2004; 14(6): 1577-1580.
16. Wang XQ, Zhao CP, Zhong LC, Zhu DL, Mai DH, Liang MG, He MH. Preparation of 4-Flexible Amino-2-Arylethenyl-Quinoline Derivatives as Multi-target Agents for the Treatment of Alzheimer's Disease. Molecules. 2018; 23(12): 3100.
17. Bawa S, Kumar S, Drabu S, Kumar R. Structural modifications of quinoline-based antimalarial agents: recent developments. Journal of Pharmacy and Bioallied Sciences. 2010; 2(2): 64-71.
18. Huang L, Lu C, Sun Y, Mao F, Luo Z, Su T, Jiang H, Shan W, Li X. Multitarget-directed benzylideneindanone derivatives: anti-β-amyloid (Aβ) aggregation, antioxidant, metal chelation, and monoamine oxidase B (MAO-B) inhibition properties against Alzheimer's disease. Journal of Medicinal Chemistry. 2012; 55(19): 8483-8492.
19. Patil V, Barragan E, Patil SA, Patil SA, Bugarin A. Direct synthesis and antimicrobial evaluation of structurally complex chalcones. Chemistry Select, 2016: 1(13): 3647-3650.
20. Katila P, Shrestha A, Shrestha A, Shrestha R, Park PH, Lee ES. Design and Synthesis of Fluorinated and/or Hydroxylated 2-Arylidene-1-indanone Derivatives as an Inhibitor of LPS-stimulated ROS Production in RAW 264.7 Macrophages with Structure–Activity Relationship Study. Bulletin of the Korean Chemical Society. 2018; 39(12): 1432-1441.
21. Adole VA, Jagdale BS, Pawar TB, Sagane AA. Ultrasound promoted stereoselective synthesis of 2,3-dihydrobenzofuran appended chalcones at ambient temperature. South African Journal of Chemistry. 2020; 73: 35-43.
22. Gomes MN, Braga RC, Grzelak EM, Neves BJ, Muratov E, Ma R, Klein LL, Cho S, Oliveira GR, Franzblau SG, Andrade CH. QSAR-driven design, synthesis and discovery of potent chalcone derivatives with antitubercular activity. European Journal of Medicinal Chemistry. 2017; 137: 126-138.
23. Avila-Villarreal G, Hernández-Abreu O, Hidalgo-Figueroa S, Navarrete-Vázquez G, Escalante-Erosa F, Peña-Rodríguez LM, Villalobos-Molina R, Estrada-Soto S. Antihypertensive and vasorelaxant effects of dihydrospinochalcone-A isolated from Lonchocarpus xuul Lundell by NO production: Computational and ex vivo approaches. Phytomedicine. 2013; 20(14): 1241-1246.
24. Faidallah HM, Rostom SA, Khan KA. Synthesis and biological evaluation of pyrazole chalcones and derived bipyrazoles as anti-inflammatory and antioxidant agents. Archives of Pharmacal Research. 2015; 38(2): 203-215.
25. Kamal A, Balakrishna M, Loka Reddy V, Riyaz S, Bagul C, Satyanarayana BM, Venkateswar Rao J. Synthesis and Biological Evaluation of Benzo [d][1,3] Dioxol-5-yl Chalcones as

Antiproliferating Agents. Chemical Biology & Drug Design. 2015; 86(5): 1267-1284.
26. Wan Z, Hu D, Li P, Xie D, Gan X. Synthesis, antiviral bioactivity of novel 4-thioquinazoline derivatives containing chalcone moiety. Molecules. 2015; 20(7): 11861-11874.
27. Moodley T, Momin M, Mocktar C, Kannigadu C, Koorbanally NA. The synthesis, structural elucidation and antimicrobial activity of 2-and 4-substituted-coumarinyl chalcones. Magnetic Resonance in Chemistry. 2016; 54(7): 610-617.
28. Chaudhari MB, Moorthy S, Patil S, Bisht GS, Mohamed H, Basu S, Gnanaprakasam B. Iron-catalyzed batch/continuous flow C–H functionalization module for the synthesis of anticancer peroxides. The Journal of Organic Chemistry. 2018; 83(3): 1358-1368.
29. Chaudhari MB, Jayan K, Gnanaprakasam B. Sn-Catalyzed Criegee-Type Rearrangement of Peroxyoxindoles Enabled by Catalytic Dual Activation of Esters and Peroxides. The Journal of Organic Chemistry. 2020; 85(5): 3374-3382.
30. Chaudhari MB, Bisht GS, Kumari P, Gnanaprakasam B. Ruthenium-catalyzed direct α-alkylation of amides using alcohols. Organic & Biomolecular Chemistry. 2016; 14(39): 9215-9220.
31. Chaudhari MB, Mohanta N, Pandey, AM, Vandana M, Karmodiya K, Gnanaprakasam B. Peroxidation of 2-oxindole and barbituric acid derivatives under batch and continuous flow using an eco-friendly ethyl acetate solvent. Reaction Chemistry & Engineering. . 2019; 4(7): 1277-1283.
32. Adole VA, Pawar TB, Jagdale BS. Aqua-mediated rapid and benign synthesis of 1,2,6,7-tetrahydro-8H-indeno[5,4-b] furan-8-one-appended novel 2-arylidene indanones of pharmacological interest at ambient temperature. Journal of the Chinese Chemical Society. 2020; 67(2): 306-315.
33. Adole VA. Synthetic approaches for the synthesis of dihydropyrimidinones/thiones (biginelli adducts): a concise review. World Journal of Pharmaceutical Research. 2020; 9(6): 1067-1091.
34. Adole VA, Pawar TB, Koli PB, Jagdale BS. Exploration of catalytic performance of nano-La2O3 as an efficient catalyst for dihydropyrimidinone/thione synthesis and gas sensing. Journal of Nanostructure in Chemistry. 2019; 9(1): 61-76.
35. Patil BN, Lade JJ, Parab AA, Sathe PA, Vadagaonkar KS, Chaskar AC. NBS-assisted an efficient conversion of styrenes to α-hydroxy ketones in water. Tetrahedron Letters. 2019; 60(27):1788-1791.
36. Lade JJ, Patil BN, Sathe PA, Vadagaonkar KS, Chetti P, Chaskar AC. Iron Catalyzed Cascade Protocol for the Synthesis of Pyrrolo [1, 2-a] quinoxalines: A Powerful Tool to Access Solid State Emissive Organic Luminophores. Chemistry Select. 2017; 2(23): 6811-6817.
37. Patil BN, Lade JJ, Pardeshi SD, Patil P, Chaskar AC. Polyethylene-Glycol-(PEG-400) Mediated Environmentally Benign Protocol for the Synthesis of Pyrrolo [1,2-a] quinoxalines from Benzyl Amines at Room Temperature. Chemistry Select. 2019; 4(38): 11362-11366.
38. Adole VA, More RA, Jagdale BS, Pawar TB, Chobe SS. Efficient synthesis, antibacterial, antifungal, antioxidant and cytotoxicity study of 2-(2-hydrazineyl) thiazole derivatives. Chemistry Select. 2020; 5(9): 2778-2786.
39. Chobe SS, Adole VA, Deshmukh KP, Pawar TB, Jagdale BS. Poly (ethylene glycol)(PEG-400): A green approach towards synthesis of novel pyrazolo [3, 4-d] pyrimidin-6-amines derivatives and their antimicrobial screening. Archives of Applied Science Research. 2014; 6(2): 61-66.
40. Parlak C, Ramasami P, Tursun M, Rhyman L, Kaya MF, Atar N, Alver Ö, Şenyel M. 4-Mercaptophenylboronic acid: Conformation, FT-IR, Raman, OH stretching and theoretical studies. Spectrochimica Acta Part A: Molecular and Biomolecular Spectroscopy. 2015; 144: 131-138.
41. Govindarasu K, Kavitha E. Molecular structure, vibrational spectra, NBO, UV and first order hyperpolarizability, analysis of 4-Chloro-dl-phenylalanine by density functional theory. Spectrochimica Acta Part A: Molecular and Biomolecular Spectroscopy. 2014; 133: 799-810.
42. Rani U, Karabacak M, Tanrıverdi O, Kurt M, Sundaraganesan N. The spectroscopic (FTIR, FT-Raman, NMR and UV), first-order hyperpolarizability and HOMO–LUMO analysis of methylboronic acid. Spectrochimica Acta Part A: Molecular and Biomolecular Spectroscopy. 2012; 92: 67-77.
43. Adole VA, Waghchaure RH, Jagdale BS, Pawar TB, Pathade SS. Molecular structure, frontier molecular orbital and spectroscopic examination on dihydropyrimidinones: a comparative computational approach. Journal of Advanced Scientific Research, 2020; 11(2): 64-70.
44. Sebastian S, Sylvestre S, Sundaraganesan N, Amalanathan M, Ayyapan S, Oudayakumar K, Karthikeyan B. Vibrational spectra, molecular structure, natural bond orbital, first order hyperpolarizability, TD-DFT and thermodynamic analysis of 4-amino-3-hydroxy-1-naphthalenesulfonic acid by DFT approach. Spectrochimica Acta Part A. Molecular and Biomolecular Spectroscopy. 2013; 107: 167-178.
45. Sawant AB, Nirwan RS. Synthesis, characterization and DFT studies of 6, 8-dichloro-2-(4-chlorophenyl)-4H-chromen-4-one. Indian Journal of Pure & Applied Physics. 2012; 50(1): 308-313,
46. Sawant AB, Gill CH, Nirwan RS. Molecular structure and vibrational spectra of 2-[5-(4-chlorophenyl)-4, 5-dihydro-1H-pyrazol-3-yl] phenol. Indian Journal of Pure & Applied Physics. 2012; 50(1): 38-44.
47. Adole VA, Waghchaure RH, Jagdale BS, Pawar TB. Investigation of Structural and Spectroscopic Parameters of Ethyl 4-(4-isopropylphenyl)-6-methyl-2-oxo-1,2,3,4-tetrahydropyrimidine-5-carboxylate: a DFT Study. Chemistry & Biology Interface. 2020; 10(1): 22-30.
48. Adole VA, Waghchaure RH, Pathade SS, Patil MR, Pawar TB, Jagdale BS. Solvent-free grindstone synthesis of four new (E)-7-(arylidene)-indanones and their structural, spectroscopic and quantum chemical study: a comprehensive theoretical and experimental exploration. Molecular Simulation. 2020; 46(14): 1045-1054.
49. Adole VA, Pawar TB, Jagdale BS. DFT computational insights into structural, electronic and spectroscopic parameters of 2-(2-Hydrazineyl) thiazole derivatives: a concise theoretical and experimental approach. Journal of Sulfur Chemistry. 2020:1-8.
50. Mohammed HK, Ayyash AN. Vibrational Spectroscopy, Molecular properties, IR, UV-Visible, NMR Spectra and (HF, DFT) Calculations of Organic Molecule. Asian Journal of Research in Chemistry. 2019;12(5):274-277.
51. Ghammamy S, Qaitmas NA, Lashgari A. Structural Properties, Natural Bond Orbital, Theory Functional Calculations (DFT), and Energies for the Two New Halo Organic Compounds. Asian Journal of Research in Chemistry. 2015;8(1):60-65.
52. Dhonnar SL, Adole VA, Sadgir NV, Jagdale BS. Structural, Spectroscopic (UV-Vis and IR), Electronic and Chemical Reactivity Studies of (3,5-Diphenyl-4, 5-dihydro-1H-pyrazol-1-yl)(phenyl) methanone. Physical Chemistry Research. 2021; 9(2): 193-209.
53. Lashgari A, Ghammamy S, Shahsavari M. Theoretical and Density Functional Theory (DFT) studies for the organic compound: 2-Amino-6-chloro-N-methylbenzamide. Asian Journal of Research in Chemistry. 2014 Jul 28;7(7):677-680.
54. Pawar TB, Jagdale BS, Sawant AB, Adole VA. DFT Studies of 2-[(2-substitutedphenyl) carbamoyl] benzoic acids. Journal of Chemical, Biological and Physical Sciences. 2017;7:167-175.
55. Hassan MF, Ayyash AN. Study of Spectral and Molecular Properties of Polyatomic molecule by Semiempirical and DFT Methods. Asian Journal of Research in Chemistry. 2019; 12(6): 330-334.
56. Adole VA, Koli PB, Shinde RA, Shinde RS. Computational Insights on Molecular Structure, Electronic Properties, and Chemical Reactivity of (E)-3-(4-Chlorophenyl)-1-(2-Hydroxyphenyl) Prop-2-en-1-one. Material Science Research India. 2020;17(special issue 2020):41-53.
57. Jayanna ND. An efficient synthesis of 2-(6-methoxy-2-napthyl)-1,

3-benzoxazole derivatives using IBD/LTA: Reactivity, DFT, Anticancer and Larvicidal activities. Asian Journal of Research in Chemistry. 2020;13(5):312-318.
58. Adole VA, Jagdale BS, Pawar TB, Desale BS. Molecular structure, frontier molecular orbitals, MESP and UV–visible spectroscopy studies of Ethyl 4-(3, 4-dimethoxyphenyl)-6-methyl-2-oxo-1,2,3,4-tetrahydropyrimidine-5-carboxylate: A theoretical and experimental appraisal. Material Science Research India. 2020;17(special issue2020):13-36.
59. Pathade SS, Adole VA, Jagdale BS, Pawar TB. Molecular structure, electronic, chemical and spectroscopic (UV-visible and IR) studies of 5-(4-chlorophenyl)-3-(3, 4-dimethoxyphenyl)-1-phenyl-4, 5-dihydro-1H-pyrazole: combined DFT and experimental exploration. Material Science Research India. 2020; 17(special issue 2020):27-40.
60. Siahgali S, Ghammamy S. Theoretical Functional Calculations (DFT) Studies of Structural Properties of 1-Benzoyl-3-[(2-benzyl Sulfanyl) phenyl] thiourea with Comparison of Experimental Data. Asian Journal of Research in Chemistry. 2014;7(1):62-66.
61. Kumari BJ, Reji TA. Spectroscopic Investigation, HOMO-LUMO and Mulliken analysis of 2-[2-(Butylamino-4-phenylaminothiazol)-5-oyl] benzothiazole by DFT study. Asian Journal of Research in Chemistry. 2017;10(6):819-826.
62. Shinde RA, Adole VA, Jagdale BS, Pawar TB, Desale BS, Shinde RS. Efficient Synthesis, Spectroscopic and Quantum Chemical Study of 2,3-Dihydrobenzofuran Labelled Two Novel Arylidene Indanones: A Comparative Theoretical Exploration. Material Science Research India. 2020;17(2):146-61.
63. Sangeetha S, Reji TF. Molecular Geometry, Vibrational Assignments, HOMO-LUMO, Mulliken's charge analysis and DFT Calculations of 2-(2-Phenylaminothiazole-5-oyl) 1-methyl-6-methylbenzimidazole. Asian Journal of Research in Chemistry. 2018; 11(6): 848-856.
64. Pokharia S. A Density Functional Theory (DFT) study on di-n-butyltin (IV) derivative of glycyltryptophane. Asian Journal of Research in Chemistry. 2016; 9(2):53-61.
65. Shinde RA, Adole VA, Jagdale BS, Pawar TB. Experimental and Theoretical Studies on the Molecular Structure, FT-IR, NMR, HOMO, LUMO, MESP, and Reactivity Descriptors of (*E*)-1-(2,3-Dihydrobenzo [*b*][1,4] dioxin-6-yl)-3-(3,4,5-trimethoxyphenyl) prop-2-en-1-one. Material Science Research India. 2020; 17(special issue 2020): 54-72.
66. Pokharia S. Theoretical insights on Organotin (IV)-protein interaction: Density Functional Theory (DFT) studies on di-n-butyltin (IV) derivative of Glycylvaline. Asian Journal of Research in Chemistry. 2015; 8(1):7-12.
67. Sawant AB, Nirwan RS. Synthesis, characterization and DFT studies of 6,8-dichloro-2-(4-chlorophenyl)-4H-chromen-4-one. Indian Journal of Pure and Applied Physics. 2012;50:308-313.
68. Nirwan RS, Sawant AB. Experimental and theoretical studies of 6,8-dichloro-2-(4-methoxyphenyl)-4H-chromen-4-one. Rasāyan Journal of Chemistry. 2011;4:613-619.
69. Sadgir NV, Dhonnar SL, Jagdale BS, Sawant AB. Synthesis, spectroscopic characterization, XRD crystal structure, DFT and antimicrobial study of (2E)-3-(2,6-dichlorophenyl)-1-(4-methoxyphenyl)-prop-2-en-1-one. SN Applied Sciences. 2020; 2(8): 1-12.
70. Sadgir NV, Dhonnar SL, Jagdale BS, Waghmare B, Sadgir C, Synthesis, Spectroscopic Characterization, Quantum Chemical Study and Antimicrobial Study of (2e)-3-(2, 6-Dichlorophenyl)-1-(4-Fluoro)-Prop-2-En-1-One. Material Science Research India. 2020; 17(3): 281-293.
71. Dhonnar SL, Jagdale BS, Sawant AB, Pawar TB, Chobe SS, Molecular structure, vibrational spectra and theortical HOMO–LUMO analysis of (E)-3,5-dimethyl-1-phenyl-4-(p-tolyldiazenyl)-1H-pyrazole by DFT method. Der Pharma Chemica. 2016; 8(17): 119-128.
72. Adole VA, Computational Chemistry Approach for the Investigation of Structural, Electronic, Chemical and Quantum Chemical Facets of Twelve Biginelli Adducts. Journal of Applied Organometallic Chemistry. 2021;1(1):29-40.
73. Adole VA, Bagul VR, Ahire SA, Pawar RK, Yelmame GB, Bukane AR, Computational chemistry: molecular structure, spectroscopic (UV-visible and IR), electronic, chemical and thermochemical analysis of 3'-phenyl-1,2-dihydrospiro[indeno[5,4-b]. Journal of Advanced Scientific Research. 2021; 12(1) Suppl 1:276-286.
74. Halim SA, Ibrahim MA. Synthesis, DFT computational insights on structural, optical, photoelectrical characterizations and spectroscopic parameters of the novel (2E)-3-(4-methoxy-5-oxo-5H-furo [3,2-g] chromen-6-yl) acrylonitrile (MOFCA). Journal of Molecular Structure. 2021;1223:129316.
75. Halim SA, Ibrahim MA. Synthesis, DFT calculations, electronic structure, electronic absorption spectra, natural bond orbital (NBO) and nonlinear optical (NLO) analysis of the novel 5-methyl-8H-benzo [h] chromeno [2,3-b][1, 6] naphthyridine-6 (5H), 8-dione (MBCND). Journal of Molecular Structure. 2017; 1130: 543-558.
76. Farag AAM, Roushdy N, Halim SA, El-Gohary NM, Ibrahim MA, Said S. Synthesis, molecular, electronic structure, linear and non-linear optical and phototransient properties of 8-methyl-1,2-dihydro-4H-chromeno [2,3-b] quinoline-4,6 (3H)-dione (MDCQD): Experimental and DFT investigations. Spectrochimica Acta Part A: Molecular and Biomolecular Spectroscopy. 2018; 191: 478-490.
77. Frisch MJ, Trucks GW, Schlegel HB, Scuseria GE, Robb MA, Cheeseman JR, Montgomery Jr JA, Vreven T, Kudin KN, Burant JC, Millam JM. Gaussian 03, Revision C. 02. Wallingford, CT: Gaussian. Inc. 2004.
78. Szafran M, Katrusiak A, Koput J, Dega-Szafran Z. X-ray, MP2 and DFT studies of the structure, vibrational and NMR spectra of homarine. Journal of Molecular Structure. 2007; 846(1-3):1-12.
79. Dereli Ö, Sudha S, Sundaraganesan N. Molecular structure and vibrational spectra of 4-phenylsemicarbazide by density functional method. Journal of Molecular Structure. 2011; 994(1-3): 379-386.